BMC Structural Biology

Research article

Crystal structural analysis of human serum albumin complexed with hemin and fatty acid

Patricia A Zunszain[1], Jamie Ghuman[1], Teruyuki Komatsu[2], Eishun Tsuchida[2] and Stephen Curry*[1]

Address: [1]Department of Biological Sciences, Imperial College London, Room 746 Huxley Building, South Kensington Campus, London SW7 2AZ, United Kingdom and [2]Advanced Research Institute for Science and Engineering, Waseda University, Tokyo 169-8555, Japan

Email: Patricia A Zunszain - p.zunszain@imperial.ac.uk; Jamie Ghuman - j.ghuman@imperial.ac.uk; Teruyuki Komatsu - teruyuki@waseda.jp; Eishun Tsuchida - eishun@mn.waseda.ac.jp; Stephen Curry* - s.curry@imperial.ac.uk

* Corresponding author

Published: 07 July 2003

BMC Structural Biology 2003, **3**:6

Received: 06 May 2003
Accepted: 07 July 2003

This article is available from: http://www.biomedcentral.com/1472-6807/3/6

Abstract

Background: Human serum albumin (HSA) is an abundant plasma protein that binds a wide variety of hydrophobic ligands including fatty acids, bilirubin, thyroxine and hemin. Although HSA-heme complexes do not bind oxygen reversibly, it may be possible to develop modified HSA proteins or heme groups that will confer this ability on the complex.

Results: We present here the crystal structure of a ternary HSA-hemin-myristate complex, formed at a 1:1:4 molar ratio, that contains a single hemin group bound to subdomain IB and myristate bound at six sites. The complex displays a conformation that is intermediate between defatted HSA and HSA-fatty acid complexes; this is likely to be due to low myristate occupancy in the fatty acid binding sites that drive the conformational change. The hemin group is bound within a narrow D-shaped hydrophobic cavity which usually accommodates fatty acid; the hemin propionate groups are coordinated by a triad of basic residues at the pocket entrance. The iron atom in the centre of the hemin is coordinated by Tyr161.

Conclusion: The structure of the HSA-hemin-myristate complex (PDB ID 1o9x) reveals the key polar and hydrophobic interactions that determine the hemin-binding specificity of HSA. The details of the hemin-binding environment of HSA provide a structural foundation for efforts to modify the protein and/or the heme molecule in order to engineer complexes that have favourable oxygen-binding properties.

Background

In the human body heme may be released into the circulation during enucleation of erythrocytes or through hemolytic injury. Free heme is immediately oxidized to the ferric state, hemin, which is potentially toxic since it may intercalate in lipid membranes and catalyze the formation of hydroxyl radicals and the oxidation of low density lipoproteins [1]. This toxicity is largely averted though the scavenging action of hemopexin, a protein that circulates in plasma (~17 μM), binds hemin with extremely high affinity (K_D < 1 pM) and transports it to various tissues – primarily liver cells – for intracellular catabolism [2].

Human serum albumin (HSA), the most abundant plasma protein (~640 μM) also has a high affinity for

hemin. The dissociation constant for the interaction was determined to be ~10 nM in a 3:5 (v/v) mix of dimethyl sulfoxide and water [3] but the interaction is likely to be even tighter in a more aqueous medium. HSA may provide a reserve binding capacity for situations when hemopexin becomes saturated. The protein is principally characterized by its remarkable ability to bind a broad range of hydrophobic small molecule ligands including fatty acids, bilirubin, thyroxine, bile acids and steroids; it serves as a solubilizer and transporter for these compounds and, in some cases, provides important buffering of the free concentration [4]. HSA also binds a wide variety of drugs in two primary sites [5,6] which overlap with the binding locations of endogenous ligands. The protein is a helical monomer of 66 kD containing three homologous domains (I-III) each of which is composed of A and B subdomains [5]. Despite the internal structural symmetry, the three domains have different capacities for binding fatty acids [7–10], thyroxine [11] and drugs [5,8,12,13]. Binding studies indicate a single site for hemin in subdomain IB [14] which corresponds to a binding site for fatty acids [8–10].

The ability of HSA to bind hemin has stimulated efforts to develop HSA-heme complexes that mimic the reversible oxygen-binding properties of heme proteins such as myoglobin and hemoglobin. One difficulty with this approach is that even if HSA-bound hemin is reduced to heme, stable and reversible oxygen binding by the complex cannot be observed (reviewed in [15,16]), because the heme binding site does not provide a molecular environment sufficiently similar to that found in myoglobin or hemoglobin. However, recent work has shown that artificial heme derivatives associate with HSA and provide significant oxygen-binding capacity [15,17–21]. Although such compounds have extensive modifications to the porphyrin ring and are not expected to bind to the protein in the same fashion as heme, they represent a promising line of inquiry for the development of artificial blood substitutes.

In order to advance our understanding of the heme-binding properties of HSA and the development of viable blood substitutes based on HSA-heme complexes, we have solved the crystal structure of a HSA-hemin-myristate complex. The structure reveals a previously undetected conformational state of the protein and provides a detailed view of the heme binding site. Our results are compared with a recently reported structure for methemalbumin [22].

Results and Discussion

Overall structure of the complex

The complex of HSA with hemin and myristate was prepared using a HSA:hemin:myristate mole ratio of 1:1:4 (Materials and Methods). The crystal structure was solved by molecular replacement and refined to a resolution of 3.2 Å. The refined model has an R_{free} value of 28.8% and good stereochemistry (Table 1). It contains a single molecule of hemin bound to the hydrophobic cavity in subdomain IB and myristates bound at six sites on the protein (Figure 1a). These correspond to fatty acid sites 2–7 which were identified in our previous work [8,9]. Fatty acid site 1 is occupied by hemin under our experimental conditions and prevents fatty acid binding by steric exclusion.

The electron density clearly indicates the binding configuration of the porphyrin ring and the two propionate groups of the bound hemin (Figure 1b), though it is possible that the molecule binds in two overlapping orientations that are related by a two-fold rotation (180°) about its centre. In either of the two orientations the propionate groups appear to be able to make the same interactions with the protein (to residues R114, H146 and K190) but the asymmetric location of the vinyl groups projecting from the hydrophobic end of the hemin molecule would occupy different positions. From the structure it appears that both configurations of the vinyl group could be accommodated within the binding pocket but may result in small adjustments of sidechains lining the pocket and of the exact position of the porphryin ring and its iron centre. Even at higher resolution, this ambiguity is not resolved [22] and it may therefore reflect a genuine degeneracy in hemin binding.

The density for the fatty acids is generally rather weak, indicating partial occupancy as would be expected given the 4:1 mole ratio of fatty acid to HSA used to prepare the complex. Although there is usually clear density to indicate the position of the fatty acid carboxylate moiety in each binding pocket, the density for the methyl end of the methylene tail is weak or absent. As a result, only the visible portion of the fatty acid tails has been included in the refined model.

Conformational changes

A surprising finding is that the HSA-hemin-myristate complex adopts a conformation that is intermediate between the structure of unliganded HSA [5,12,23] and that observed previously for HSA-fatty acid complexes [8–10]. The structural changes associated with fatty acid binding in previous work can be regarded essentially as rigid-body rotations of domains I and III relative to II that pivot around the mid-point of the long inter-domain helices (Figures 2a and 2b) and are driven primarily by binding of fatty acids to the I-II and II-III interfaces, though contacts between domains I and III may also be involved [8,24]. This conformational change appears to be independent of the length or degree of unsaturation of the fatty acid methylene tail [9,10] though it must be borne in

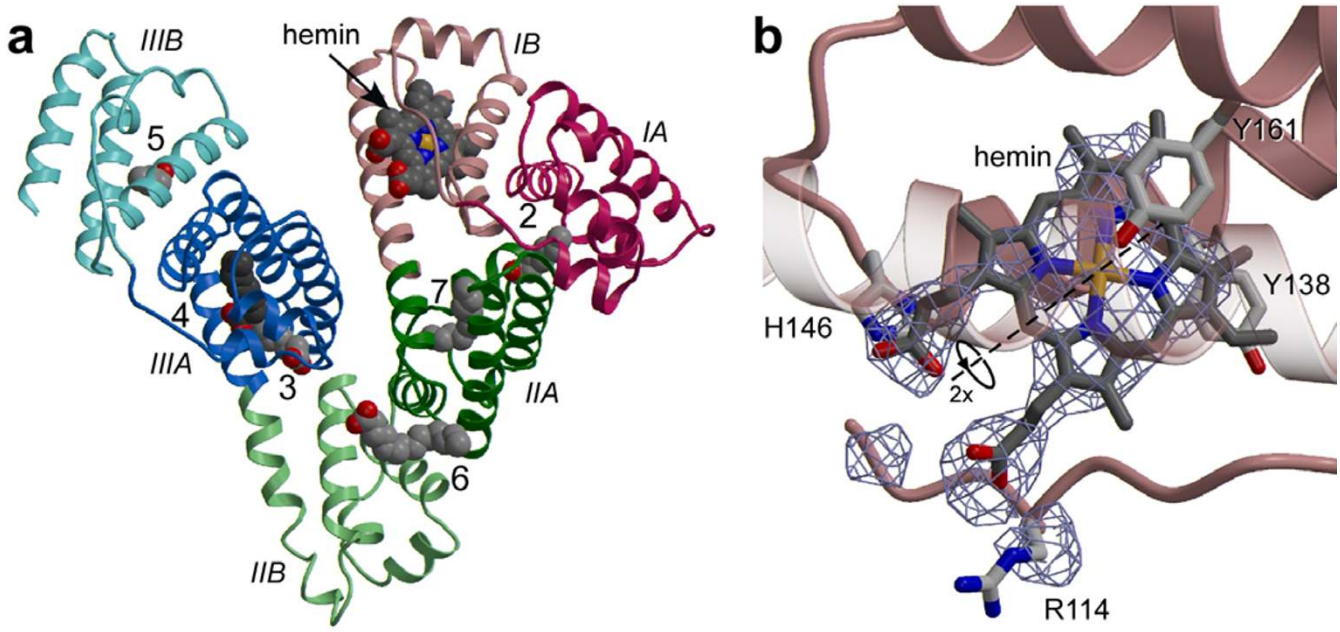

Figure 1

Crystal structure of the HSA-myristate-hemin complex (a) The protein secondary structure is shown schematically with the sub-domains colour-coded as follows: IA, red; IB – light red; IIA, green; IIB – light-green; IIIA, blue; IIIB – light blue; this colour scheme is maintained throughout. Ligands are shown in a space-filling representation, coloured by atom type: carbon – grey; nitrogen – blue; oxygen – red; iron – orange. Fatty acid binding sites are labelled 2–7. Except where stated otherwise, molecular graphics were prepared using Bobscript [32] and Raster3D [33]. **(b)** An F_{obs}-F_{calc} simulated annealing omit map [30] contoured at 2.5σ for hemin bound to subdomain IB. Selected amino acid sidechains are shown coloured by atom type. The dashed line indicates the two-fold symmetry axis that may relate alternative binding configurations of the porphyrin ring. The helix which overlies the bound hemin (residues 174–196) has been rendered semi-transparent.

mind that in these studies HSA-fatty acid complexes were prepared for crystallisation using a large molar excess of fatty acid to protein (>10:1) [9,10]. For the present investigation a 1:1 HSA-hemin complex was incubated with 4 moles of myristate per mole of HSA and then concentrated in a single step prior to crystallisation (see Materials and Methods). The crystals obtained belong to space-group $P2_12_12$, which has not previously been observed for HSA and was an early indication of the potential novelty of the conformational state. As observed for HSA-fatty acid complexes, the conformation of the HSA-hemin-myristate complex comprises changes from the unliganded state involving rigid-body rotations of domains I and III with respect to domain II; however in this case the particular rotation of domain I relative to domain II is only about 85% complete when compared to that observed in other HSA-fatty acid complex structures (Figures 2a and 2b). The difference in the orientation of domain III relative to domain II in the HSA-hemin-myristate and other HSA-fatty acid complexes [8–10,24] is rather small and may be due to differences in crystal packing.

It is conceivable that the difference in the orientation of domain I relative to domain II in the HSA-hemin-myristate and other HSA-fatty acid complexes is also due to changes in the crystal-packing environment between the two crystal forms ($P2_12_12$ and C2). However, consideration of the structure suggests that it is more likely to be due to differences in the level of bound fatty acid (Figures 2c and 2d). The crystal structure of the HSA-myristate complex – prepared using a high myristate:HSA mole ratio – showed evidence for two fatty acid molecules bound in a tail-to-tail configuration in the contiguous fatty acid sites 2 and 2' which straddle the interface between domains I and II. Occupancy of site 2 is believed to be primarily responsible for driving the conformational change between these two domains (Figure 2d). In the HSA-hemin-myristate complex, there is no evidence for fatty acid binding to site 2' and indeed the density for the fatty acid bound to site 2 is relatively weak, probably as a

result of the reduced occupancy (Figure 2c). Thus it may be that binding to site 2' is required to drive the more extensive conformational change between domains I and II. Although fatty acids longer than C14 are not observed to occupy site 2', they nevertheless appear to drive the "full" conformational change; this is most likely because the methylene tail of a long-chain fatty acid bound to site 2 begins to occupy site 2' [9,10] and may therefore play the same structural role as the binding of a second molecule of a shorter-chain fatty acid to site 2'. An independent crystallographic study on hemin binding to HSA in the presence of myristate reportedly obtained a conformation very similar to that found for HSA-myristate at very high myristate:HSA mole ratios [8], but the amount of myristate used was not given and the coordinates are not yet available to allow a direct comparison with our present structure [22]. Whatever the precise mechanism underlying the fatty-acid induced conformational changes, there is no evidence to suggest a connection between binding of hemin and the new conformational stage identified in the present work. Moreover, it is likely that the hemin-binding site itself is not affected by fatty acid induced conformational changes.

Table 1: Data collection and refinement statistics

DATA COLLECTION	
a (Å)	80.08
b (Å)	202.70
c (Å)	39.37
Resolution range (Å)	27.2–3.2
Independent reflections	10,825
Multiplicity[1]	2.7(2.6)
Completeness (%)	96.2(92.4)
I/σ	8.1(2.1)
R_{merge}(%)[2]	5.7(34.5)
MODEL REFINEMENT	
Nonhydrogen atoms	4479
R_{model} (%)[3]	28.8
R_{free} (%)[4]	23.1
r.m.s deviation from ideal bond lengths (Å)	0.007
r.m.s deviation from ideal angles (°)	1.4
Average B-factor (Å²)	75.3
PBD ID	1o9x

[1]Values for the outermost resolution shell are given in parentheses. [2] $R_{merge} = 100 \times \sum_h \sum_j |I_{hj} - I_h| / \sum_h \sum_j I_{hj}$ where I_h is the weighted mean intensity of the symmetry related reflections I_{hj} [3] $R_{model} = 100 \times \sum_{hkl} |F_{obs} - F_{calc}| / \sum_{hkl} F_{obs}$ where I_h where F_{obs} and F_{calc} are the observed and calculated structure factors respectively. [4] R_{free} is the R_{model} calculated using a randomly selected 5% sample of reflection data omitted from the refinement.

Details of the hemin binding site

Hemin binds to a hydrophobic, D-shaped cavity in subdomain IB. The hydrophobic porphyrin ring is essentially buried in the core of the subdomain with the propionate groups located at the wide entrance to the pocket where they can interact with solvent and several basic amino acid sidechains (see below). In the absence of ligand this cavity is partially occluded by two tyrosine residues (138 and 161) which stack on top of one another [24]. Upon hemin binding both sidechains undergo χ_1 rotations of around 90° thereby opening up the binding pocket and helping to clamp the ligand in place. Very similar rotations of these sidechains were observed with fatty acid binding [9]; indeed there is complete overlap between the positions of fatty acid and hemin when bound in this site. Other sidechains, including Leu139, His146, Ile142 and Leu154, exhibit modest adjustments upon heme binding.

There is a slight expansion of subdomain IB upon binding of hemin: the separation of helices 8 and 10 on either side of the ligand increases by about 1.4 Å. A similar sized expansion was also observed for fatty acid binding to this pocket [8]. The expansion may be constrained by the disulfide bridge between Cys124 and Cys169 that links helices 7 and 9 respectively (Figure 3a).

All of the structural components of subdomain IB, including the polypeptide linker connecting it to subdomain IA and helices 7–10, contribute to the hemin binding site. The hemin group binds with its plane oriented at about 30° to the directional axes of helices 8–10; this orientation is determined by the packing of the hemin group against the residues lining the interior wall of the pocket. With the exception of Tyr138 and Tyr161, these are entirely hydrophobic sidechains. The hydroxyl group of Tyr138 is relocated to the exterior of the domain where it interacts with solvent, but the hydroxyl group of Tyr161 makes a direct interaction with the central Fe^{3+} atom, providing a fifth point of coordination (Figure 3b). The entrance to the pocket, which is rather open, faces towards the interdomain cleft and contains three basic residues that coordinate the two propionate groups on hemin. Lys190 adopts a central position and makes salt-bridges to both propionate groups (2.7 and 3.0 Å); His146 provides a second electrostatic interaction with one heme carboxylate (3.0 Å) while the guanidinium group of Arg114 interacts with the other (2.8 Å). Arg117, which lies towards the top end of the pocket entrance and invariably interacts with fatty acids which bind at this site [9], is not involved in coordinating the propionate groups of the hemin. The electrostatic interactions to the propionate groups are clearly important for hemin binding; the number of residues involved in coordinating the propionate groups is fewer that the seven observed in hemopexin [25] but more than the one or two basic residues found to fill this

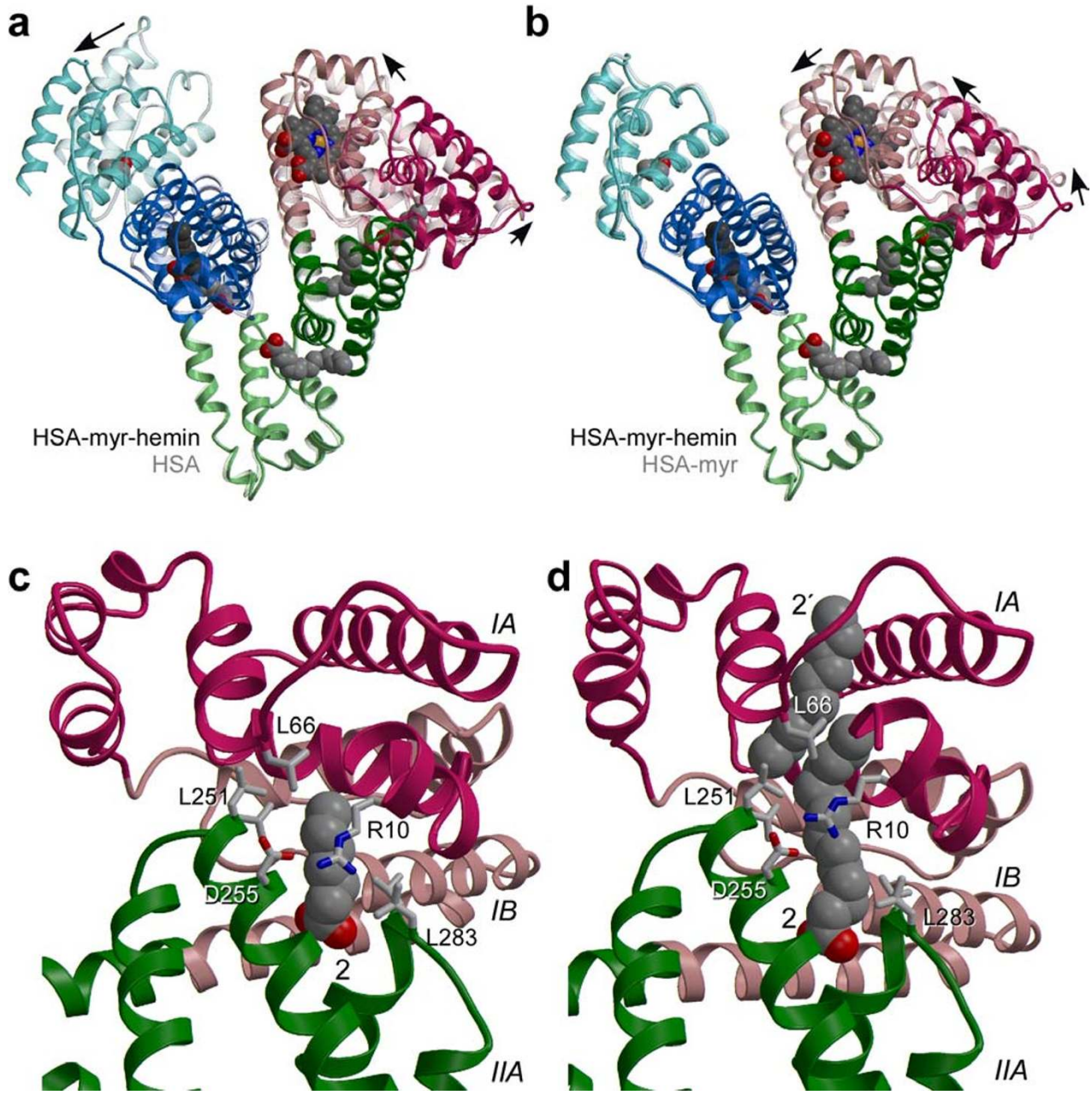

Figure 2

Conformational changes associated with variations in fatty acid content (a) Superposition of HSA-hemin-myristate (opaque) on defatted HSA (semi-transparent). **(b)** Superposition of HSA-hemin-myristate (opaque) on HSA-myristate (semi-transparent). HSA-hemin-myristate was prepared with a 4-fold molar excess of fatty acid whereas the HSA-myristate complex was prepared with a 12-fold molar excess [9] which saturates the binding sites. The colour scheme is the same as Figure 1. In each case the structures were superposed using the C_α atoms from domain II (residues 197–383). Arrows indicate the relative domain movements. **(c)** Close-up views of myristate binding site 2 which traverses the interface between domains I and II for HSA-hemin-myristate. Selected amino acid sidechains are shown coloured by atom type. The fatty acid is depicted in a space filling-representation. Only the first seven carbon atoms of the methylene tail for which there is clear electron density are shown; the remainder of the tail is disordered but presumable extends further upward. **(d)** A similar close-up view of the same site in the HSA-myristate structure [9]. In this case the site is occupied by two fatty acid molecules in a tail-to-tail configuration. The upper part of fatty acid site 2 is labelled 2'. The additional relative movement of the two domains at the higher fatty acid concentration is evident from the relative dispositions of R10 and D255, which interact across the top of the bound fatty acid.

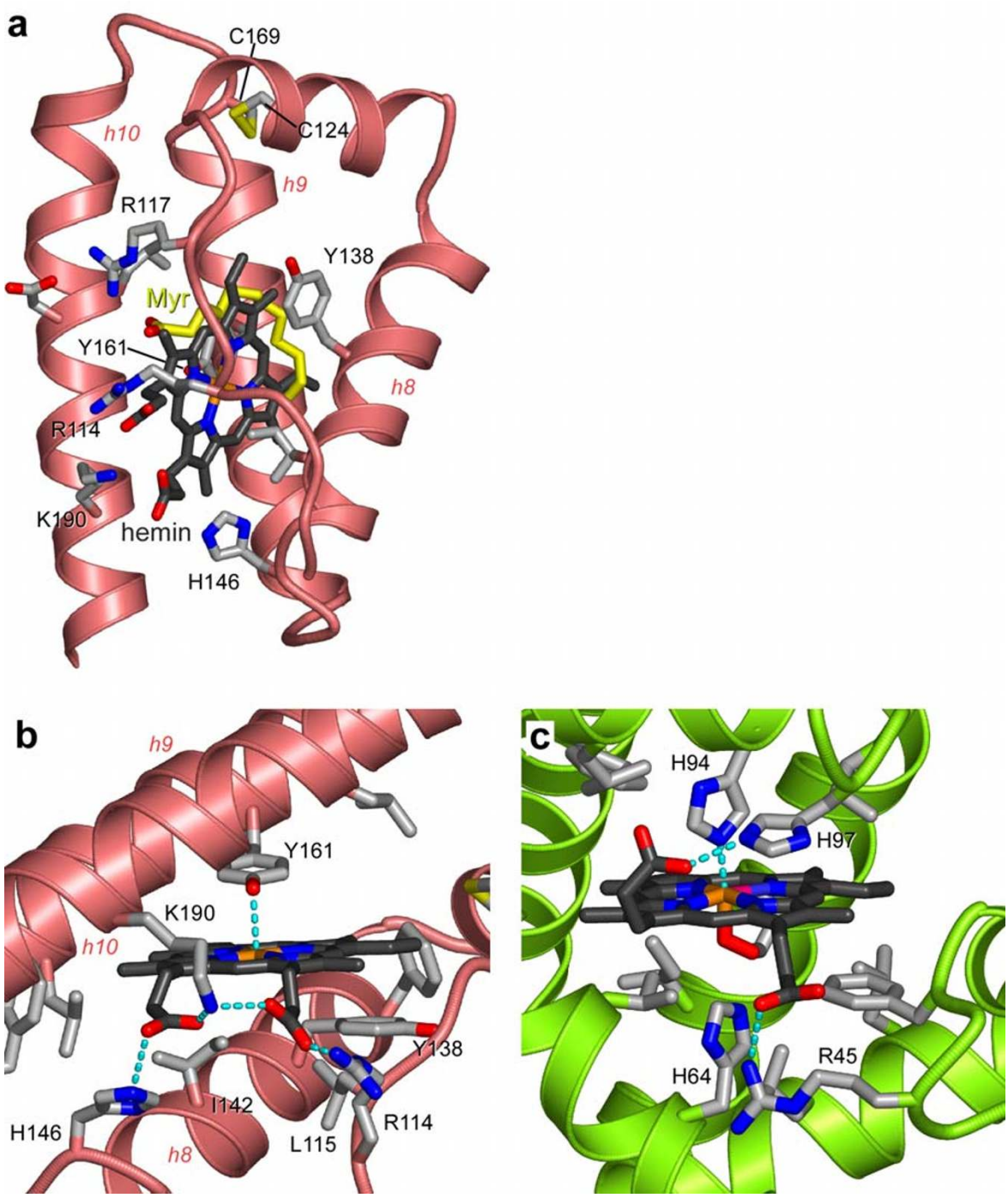

Figure 3

Detailed structure of the hemin-binding site in HSA and comparison with myoglobin (a) Side-view of subdomain IB of HSA indicating the comparative binding configurations of hemin (grey carbon atoms) and myristate (yellow carbon atoms). Helices 8–10 are labelled h8-h10. The structures of HSA-hemin-myristate and HSA-myristate [9] were superposed using the C_α atoms of subdomain IB (residues 107–196). The myristate lies along the upper hydrophobic surface of the D-shaped cavity that accommodates hemin. Note that R117, which serves to coordinate the carboxylate group of myristate, is not involved in this function for hemin. **(b)** Close-up view of the hemin-binding pocket in subdomain IB. The propionate groups of hemin are co-ordinated by R114, H146 and K190. **(c)** Close-up view of the heme-binding pocket of sperm-whale myoglobin (PDB ID: 4 mbn). Electrostatic interactions between protein side-chains and hemin are indicated by dashed cyan lines. This figure was prepared using Molscript [34] and Pymol [35].

role in myoglobin or hemoglobin (Figure 3c). At the opposite end of the pocket there is a small opening which is large enough to admit solvent molecules.

In terms of the general hydrophobicity of the pocket and the coordination of the propionate groups by basic residues, HSA appears to have similar features to the heme binding site on myoglobin or hemoglobin. However, although both proteins are helical there is little similarity in the architectures of their heme binding pockets. In particular, HSA lacks the pair of histidine residues that serve to enhance and regulate the relative oxygen- and carbon monoxide-binding properties of myoglobin and hemoglobin. Modification of the heme-binding pocket on HSA or of the heme-group itself is likely to be required to achieve a protein-heme complex capable of reversible oxygen binding. Although various heme derivatives have been produced that exhibit reversible oxygen binding in association with HSA [19–21,26], these contain sizeable additions to the porphyrin ring structure and are unlikely to bind to subdomain IB on HSA in the same configuration that has been observed for hemin. Nevertheless, the detailed architecture of the heme-binding pocket as revealed by this crystallographic study will facilitate the design of new heme derivatives that will be better accommodated in this site and may therefore bind with higher affinity. It will also enable the design of mutagenesis experiments to tailor the pocket to bind modified hemes.

Conclusions

The structure of the HSA-hemin-myristate complex reported here reveals a new conformational state of the protein, one that is intermediate between unliganded HSA and the saturated HSA-fatty acid complex. The observation of this conformation is likely due to the use of subsaturating amounts of fatty acid in preparing the crystals and provides new insights into the mechanism of conformational change.

The single hemin-binding pocket in subdomain IB of HSA consists of a deep hydrophobic slot that provides three basic residues at its entrance to coordinate the two propionate groups of the hemin. This provides a framework for future attempts to engineer the protein and heme derivative in order to generate high-affinity HSA-heme complexes which bind oxygen reversibly and may serve as effective artificial blood substitutes.

Methods

Preparation and crystallization of the HSA-hemin-myristate complex

Recombinant HSA (Recombin®), kindly provided by Delta Biotechnology (Nottingham, UK), was defatted and purified by gel filtration to be dimer-free in 50 mM potassium phosphate, 50 mM NaCl, pH 7.0 to a concentration of 110 mg/ml (1.67 mM) essentially as described previously [12]. Immediately prior to use hemin was dissolved at 10 mM in dimethylsulfoxide (DMSO) in a foil-wrapped microcentrifuge tube. The hemin and HSA solutions were mixed to give a hemin:HSA molar ratio of 1.1 to 1.0, and incubated with rotation in the dark at room temperature for at least 12 hours. The resulting complex was then concentrated using a 10 kDa molecular weight cut-off ultrafiltration device (Vivaspin, Millipore), and washed in repeated cycles of concentration and dilution with 50 mM potassium phosphate buffer, pH 7.0 to reduce the final concentration of DMSO < 0.1% (v/v). Myristic acid was freshly dispersed with the aid of mild heating in 20 mM potassium phosphate pH 7.0 to obtain a suspension with a concentration of 2.5 mM. The HSA-hemin complex was incubated with myristic acid, at a fatty acid:HSA molar ratio of 4:1, by rotation at room temperature for one hour. The complex was then concentrated – in a single step – in a Vivaspin ultrafiltration device and analysed on a polyacrylamide gel to estimate the protein concentration.

Crystals were grown by sitting-drop vapour diffusion at 4°C using methods similar to those described previously [8,9,27]. Crystallization screens were set up at a protein concentration of >90 mg/ml using 20 to 40% PEG 3350 (Sigma-Aldrich) in 50 mM potassium phosphate buffer, pH 7.0 as the precipitant; the sitting drop initially contained 3.5 μl of the protein solution and 3.5 μl of the reservoir mixture. Three days after streak-seeding, crystals were observed at 24, 26, 28 and 30% PEG; the largest crystals were observed at 24 and 26 % PEG.

Data collection, processing, structure determination and refinement

X-ray diffraction data were collected at Daresbury SRS (station 9.6) and EMBL/DESY Hamburg (beamline X11) using crystals mounted in sealed glass capillaries maintained at room temperature. The data were indexed and measured with MOSFLM and scaled with SCALA [28]. The crystals belong to space-group $P2_12_12$. Efforts to solve the phase problem by molecular replacement with AMoRe [29] produced a promising solution for domain II of the protein (residues 197–383) taken from the HSA-myristate structure (PDB ID 1e7g) [9]; however, orientations for domains I and III were not found. Since the solution for domain II appeared to yield a sensible packing arrangement for HSA molecules in the unit cell, it was used as a starting point for rigid-body refinement using CNS [30]. The HSA-myristate model (1e7g) was initially refined as a single rigid body using data from 10–30 Å; thereafter, the protein was split into three domains (5–196, 197–383, 384–584) which were allowed to move independently and rigid body refinement was applied as the high resolution limit of the incorporated data was extended in 1 Å steps from 10 Å to 4 Å and finally to 3.2 Å. During this

process, the R_{free} (defined in table 1) dropped from 51.3% to 34.5%. An electron density map calculated at this stage showed clear electron density for the whole protein and the ligand molecules. Manual building in O [31] was interspersed with rounds of positional and group temperature factor refinement. Data collection and refinement statistics are summarized in Table 1.

Authors' contributions

PZ prepared and crystallized the complex and participated in data collection and processing. JG obtained the initial crystallisation conditions for HSA-myristate-hemin complexes and assisted with data collection. ET and TK participated in the design of the study and advised on hemin handling. SC participated in the design and coordination of the study, assisted in data collection and processing, refined the structure and drafted the manuscript. All authors read and approved the final manuscript.

Acknowledgements

We thank Delta Biotechnology (UK) for providing purified recombinant HSA (Recombumin®). We are indebted to the staff at Daresbury SRS (station 9.6) and EMBL/DESY Hamburg (X11) for assistance with data collection. JG is grateful for the award of an MRC studentship. This work was funded with grant support from the BBSRC (SC) and partially supported by the Health Science Research Grants (Research on Pharmaceutical and Medical Safety) for the MHLW.

References

1. Jeney V, Balla J, Yachie A, Varga Z, Vercellotti GM, Eaton JW and Balla G: **Pro-oxidant and cytotoxic effects of circulating heme** *Blood* 2002, **100:**879-887.
2. Tolosano E and Altruda F: **Hemopexin: structure, function, and regulation** *DNA Cell Biol* 2002, **21:**297-306.
3. Adams PA and Berman MC: **Kinetics and mechanism of the interaction between human serum albumin and monomeric haemin** *Biochem J* 1980, **191:**95-102.
4. Peters T: **All about albumin: biochemistry, genetics and medical applications** *San Diego, Academic Press*; 1995.
5. He XM and Carter DC: **Atomic structure and chemistry of human serum albumin** *Nature* 1992, **358:**209-215.
6. Sudlow G, Birkett DJ and Wade DN: **The characterization of two specific drug binding sites on human serum albumin** *Mol Pharmacol* 1975, **11:**824-832.
7. Hamilton JA, Era S, Bhamidipati SP and Reed RG: **Locations of the three primary binding sites for long-chain fatty acids on bovine serum albumin** *Proc Natl Acad Sci USA* 1991, **88:**2051-2054.
8. Curry S, Mandelkow H, Brick P and Franks N: **Crystal structure of human serum albumin complexed with fatty acid reveals an asymmetric distribution of binding sites** *Nature Structural Biology* 1998, **5:**827-835.
9. Bhattacharya AA, Grüne T and Curry S: **Crystallographic analysis reveals common modes of binding of medium and long-chain fatty acids to human serum albumin** *J Mol Biol* 2000, **303:**721-732.
10. Petitpas I, Grüne T, Bhattacharya AA and Curry S: **Crystal structures of human serum albumin complexed with monounsaturated and polyunsaturated fatty acids** *J Mol Biol* 2001, **314:**955-960.
11. Petitpas I, Petersen CE, Ha CE, Bhattacharya AA, Zunszain PA, Ghuman J, Bhagavan NV and Curry S: **Structural basis of albumin-thyroxine interactions and familial dysalbuminemic hyperthyroxinemia** *Proc Natl Acad Sci USA* 2003, **100:**6440-6445.
12. Bhattacharya AA, Curry S and Franks NP: **Binding of the general anesthetics propofol and halothane to human serum albumin: high-resolution crystal structures** *J Biol Chem* 2000, **275:**38731-38738.
13. Petitpas I, Bhattacharya AA, Twine S, East M and Curry S: **Crystal structure analysis of warfarin binding to human serum albumin: anatomy of drug site 1** *J Biol Chem* 2001, **276:**22804-22809.
14. Dockal M, Carter DC and Ruker F: **The three recombinant domains of human serum albumin. Structural characterization and ligand binding properties** *J Biol Chem* 1999, **274:**29303-29310.
15. Tsuchida E, Ando K, Maejima H, Kawai N, Komatsu T, Takeoka S and Nishide H: **Properties of and oxygen binding by albumin- tetraphenylporphyrinatoiron(II) derivative complexes** *Bioconjug Chem* 1997, **8:**534-538.
16. Marden MC, Hazard ES, Leclerc L and Gibson QH: **Flash photolysis of the serum albumin-heme-CO complex** *Biochemistry* 1989, **28:**4422-4426.
17. Komatsu T, Hamamatsu K, Takeoka S, Nishide H and Tsuchida E: **Human serum albumin-bound synthetic hemes as an oxygen carrier: determination of equilibrium constants for heme binding to host albumin** *Artif Cells Blood Substit Immobil Biotechnol* 1998, **26:**519-527.
18. Komatsu T, Matsukawa Y and Tsuchida E: **Kinetics of CO and O2 binding to human serum albumin-heme hybrid** *Bioconjug Chem* 2000, **11:**772-776.
19. Tsuchida E, Komatsu T, Hamamatsu K, Matsukawa Y, Tajima A, Yoshizu A, Izumi Y and Kobayashi K: **Exchange transfusion with albumin-heme as an artificial O2-infusion into anesthetized rats: physiological responses, O2-delivery, and reduction of the oxidized hemin sites by red blood cells** *Bioconjug Chem* 2000, **11:**46-50.
20. Tsuchida E, Komatsu T, Matsukawa Y, Nakagawa A, Sakai H, Kobayashi K and Suematsu M: **Human serum albumin incorporating synthetic heme: Red blood cell substitute without hypertension by nitric oxide scavenging** *J Biomed Mater Res* 2003, **64A:**257-261.
21. Tsuchida E, Komatsu T, Matsukawa Y, Hamamatsu K and Wu J: **Human serum albumin incorporating Tetrakis(o-pivalamido) phenylporphinatoiron(II) derivative as a totally synthetic O2-carrying hemoprotein** *Bioconjug Chem* 1999, **10:**797-802.
22. Wardell M, Wang Z, Ho JX, Robert J, Ruker F, Ruble J and Carter DC: **The atomic structure of human methemalbumin at 1.9 Å** *Biochem Biophys Res Commun* 2002, **291:**813-819.
23. Sugio S, Kashima A, Mochizuki S, Noda M and Kobayashi K: **Crystal structure of human serum albumin at 2.5 Å resolution** *Protein Eng* 1999, **12:**439-446.
24. Curry S, Brick P and Franks NP: **Fatty acid binding to human serum albumin: new insights from crystallographic studies** *Biochim Biophys Acta* 1999, **1441:**131-140.
25. Paoli M, Anderson BF, Baker HM, Morgan WT, Smith A and Baker EN: **Crystal structure of hemopexin reveals a novel high-affinity heme site formed between two beta-propeller domains** *Nat Struct Biol* 1999, **6:**926-931.
26. Komatsu T, Matsukawa Y and Tsuchida E: **Effect of heme structure on O2-binding properties of human serum albumin-heme hybrids: intramolecular histidine coordination provides a stable O2-adduct complex** *Bioconjug Chem* 2002, **13:**397-402.
27. Carter DC, Chang B, Ho JX, Keeling K and Krishnasami Z: **Preliminary crystallographic studies of four crystal forms of serum albumin** *Eur J Biochem* 1994, **226:**1049-1052.
28. Collaborative Computer Project No. 4.: **The CCP4 suite: programs for protein crystallography** *Acta Crystallogr.* 1994, **D50:**760-763.
29. Navaza J: **Implementation of molecular replacement in AMoRe** *Acta Crystallogr.* 2001, **D57:**1367-1372.
30. Brünger AT, Adams PD, Clore GM, DeLano WL, Gros P, Grosse-Kunstleve RW, Jiang JS, Kuszewski J, Nilges M, Pannu NS, Read RJ, Rice LM, Simonson T and Warren GL: **Crystallography & NMR system: A new software suite for macromolecular structure determination** *Acta Crystallogr.* 1998, **D54:**905-921.
31. Jones TA, Zou JY, Cowan SW and Kjeldgaard M: **Improved methods for building protein models in electron density maps and the location of errors in these maps** *Acta Crystallogr.* 1991, **A47:**110-119.
32. Esnouf R: **An extensively modified version of Molscript that includes greatly enhanced colouring capabilities** *J Mol Graphics* 1997, **15:**133-138.

33. Merrit EA and Bacon DJ: **Raster3D - photorealistic molecular graphics** *Methods in Enzymology* 1997, **277:**505-524.
34. Kraulis PJ: **MOLSCRIPT: a program to produce both detailed and schematic plots of protein structures** *J App Crystallogr* 1991, **24:**946-950.
35. Delano WL: **The PyMOL molecular graphics system** *San Carlos, CA, USA, DeLano Scientific*; 2002.